Current tectonics of the Richardson Mountains, northwestern Canada, from preliminary double-difference earthquake relocations

Andrew J. Schaeffer and Jeremy M. Gosselin*
Natural Resources Canada, Geological Survey of Canada - Pacific

Pascal Audet
University of Ottawa

John F. Cassidy
Natural Resources Canada, Geological Survey of Canada - Pacific

Collin Paul
Natural Resources Canada, Canadian Hazards Information Service

Schaeffer, A.J., Gosselin, J.M., Audet, P., Cassidy, J.F. and Paul, C., 2026. Current tectonics of the Richardson Mountains, northwestern Canada, from preliminary double-difference earthquake relocations. *In*: Yukon Exploration and Geology 2025, A. Stuart, L.H. Weston and S.K. Schultz (eds.), Yukon Geological Survey, Government of Yukon, p. 149–165.

Abstract

The Richardson Mountains (RM) of northwestern Canada form a tectonically active boundary between the northern Canadian Cordillera and stable North American craton. Although host to abundant seismicity, the RM modern geometry and kinematics remain poorly resolved. To better delineate active structures, we apply double-difference (DD) earthquake relocation to all seismicity in the Canadian National Earthquake Database (NEDB) between 2015 and 2021 (775 events). We jointly invert catalogue P and S-wave picks and waveform cross-correlation measurements with the *scrtdd* implementation of *HypoDD*.

The resulting 594-event catalogue reveals two zones. Along the eastern front of the central RM, DD relocations collapse into a sharply defined west-dipping plane extending from the surface to 35 km. Its approximate 75° dip and surface intersection with the Knorr fault suggest that contemporary deformation is reactivating a Paleozoic normal fault. In contrast, seismicity remains broadly distributed across the White Mountains and Barn uplifts, reflecting deformation partitioned among several interacting inherited structures within a complex deformation zone. A reduction in seismicity between these regions (in both original and relocated catalogues) may indicate structural segmentation or a locked segment with implications for seismic hazard.

These results demonstrate the effectiveness of DD relocation for resolving active tectonic structures in remote northern regions and provide a refined framework for future investigations. Continued incorporation of new data from the Western Arctic Regional Network of Seismographs (WARNS) will support improved assessments of crustal deformation and seismic hazard in Canada's North.

* andrew.schaeffer@nrcan-rncan.gc.ca

Plain language summary

The Richardson Mountains in northwestern Canada are situated at the junction between two very different parts of the continent: an active mountain belt to the west and a much older, stable region to the east. This area experiences many small earthquakes and has also produced large ones in the past, but the exact locations and behaviours of the faults that cause these earthquakes are not well understood. To improve this picture, we re-examined recent earthquakes recorded between 2015 and 2021 using methods that more precisely determine where each earthquake occurred. Out of hundreds of events, we were able to sharpen the locations of nearly 600 earthquakes. These improved locations reveal two main zones of activity. In the central Richardson Mountains, many earthquakes line up on a single, steeply sloping surface that reaches down to 35 km. This surface lines up with an ancient fault that originally formed hundreds of millions of years ago, suggesting that old structures in the region are being reactivated today. Farther north, earthquakes are more spread out. This pattern suggests that the deformation is spread over several older fault systems rather than along one main fault. Overall, this study provides a clearer picture of how the Richardson Mountains continue to deform and sets the stage for better understanding earthquake hazards in northern Canada.

Introduction

The Richardson Mountains (RM) represent a significant structural domain within the northern Canadian Cordillera (NCC), forming a narrow, north-trending range that marks the eastern limit of Cordilleran deformation in northern Yukon and the Northwest Territories (Hyndman et al., 2005b; Pinet, 2021), where they are juxtaposed to the stable North American craton. The formation and subsequent tectonic evolution of the RM are intrinsically linked to the development of the Beaufort Sea and the Canada Basin, reflecting a long history that began with continental rifting and culminated in complex Cenozoic strain transfer stemming from interactions along the Pacific margin (Mazzotti and Hyndman, 2002; Estève et al., 2022). Today, the RM region is tectonically active and hosts abundant earthquake activity. This seismicity not only presents valuable information that can enable a new understanding of the geological history and potential of the region, but also clearly identifies natural hazards to Canada's northern communities and development. In this work, we re-examine the modern earthquake catalogue across the RM region with the aim of precisely identifying reactivated structures. This is achieved using the double-difference (DD) relocation technique.

Tectonic Setting

The geological roots of the RM originate in the Richardson Trough (RT), a key paleogeographic feature that formed on the ancestral northwestern margin of Laurentia (Cecile et al., 1997; Eyster et al., 2017; Strauss et al., 2020). The RT is widely recognized as a rift basin on the southern margin of an ancestral Iapetus Ocean (Lane, 2007; Cecile et al., 2022), and specifically as a failed arm (aulacogen) of a triple rift system that developed during the early Paleozoic (Jeletsky, 1962; Cecile et al., 1997).

This trough separated the Yukon block (a basement high with relatively stable cratonic area to the west) from the Mackenzie/Peel Platform to the east (Morrow, 1999 ; Strauss et al., 2020). The RT experienced two major rift cycles that spanned the late Early Cambrian to early Middle Devonian (Cecile et al., 2022). For relevant geological maps and diagrams, see Figure 1 of Strauss et al. (2020) and Figures 1 and 2 of Cecile et al. (2022). The first cycle involved rifting from late-Early to middle-Late Cambrian, followed by post-rift subsidence lasting until the late Early Ordovician; the second cycle involved rifting from late Early Ordovician to Early Silurian, followed by post-rift subsidence lasting until the early Middle Devonian (Cecile et al., 2022). The trough accumulated a thick succession of deep-water sedimentary rocks, up to 3 km thick in the centre of the basin compared to 1 km on adjoining platforms (Cecile et al., 2022), known as the Road River Group, which ranges in age from the Late Cambrian to the early Middle Devonian (Strauss et al., 2020). This deep-water depositional setting, characterized by fine-grained carbonate and siliciclastic strata, has been compared in size and geometry to segments of the modern East African rift system, such as the Kenya Rift (Cecile et al., 1997; Cecile et al., 2022).

The modern Richardson Mountains correspond to the Richardson anticlinorium, a broad, gently north-plunging structure that resulted from the structural inversion of the RT (Pinet, 2021; Cecile et al., 2022). This inversion primarily occurred during the Late

Cretaceous to early Tertiary Laramide orogeny (Norris, 1985; Lane, 1996; Pinet, 2021), driven by east-directed compression associated with Cordilleran tectonics (Lane, 1996, 1998).

In Figure 1, we illustrate the modern configuration of the Yukon and westernmost Northwest Territories, including seismicity (yellow circles), major faults (dotted lines), defined faults (light grey lines) and the dominant terrane assemblages of Nelson et al. (2013). The RM are cut by the Richardson fault system (RFS), a major system of north-trending, curviplanar, near-vertical faults (Norris, 1985; Pinet, 2021). This array extends for nearly 600 km, originating in the Mackenzie Mountains and projecting north toward the Beaufort Sea (Gabrielse, 1991; Norris, 1997). The RFS accommodated early Paleozoic dextral strike-slip movement (Norris, 1985), but the subsequent Tertiary inversion involved primarily dip-slip reactivation and shortening (Norris, 1985; Lane, 1996).

The RM and their fault systems are critical elements in the regional tectonic framework that includes the Beaufort Sea and the origin of the Amerasia Basin (Canada Basin). Mesozoic rifting in Arctic North America led to the formation of the Canada Basin during the Jurassic–Cretaceous (Shephard et al., 2013; Faehnrich et al., 2025). Tectonic models for this opening involve counterclockwise rotation or translation of the Arctic Alaska terrane (Lane, 1997; Faehnrich et al., 2025).

Northward, the RFS is inferred to connect with fault systems defining the continental margin, potentially linking to the Husky Lakes fault system (HLFS; previously Eskimo Lakes fault zone) via the Bug Creek and Donna River faults (Lane, 1998; Pinet, 2021). The HLFS originated as a listric normal fault during the Late Jurassic–Early Cretaceous rifting (Stephenson et al., 1994; Lane, 1998). Later, tertiary contractional deformation inverted these extensional structures, contributing to the formation of the Beaufort foldbelt (Lane and Dietrich, 1995). Seismic data show that the Tertiary deformation front on the eastern side of the Richardson anticlinorium consists of a series of thrust faults, folds, and back thrusts, concentrated where Paleozoic platform carbonates transition into basinal shale (Rohr et al., 2011).

The Late Cretaceous–Tertiary deformation that inverted the RT was closely related to the subsequent formation of the Beaufort Sea fold and thrust belt (BSFTB), which extends offshore into the Beaufort-Mackenzie Basin (Lane, 2002 ; Estève et al., 2022), as indicated offshore in Figure 1. This fold belt resulted from east-west shortening caused by the collision of Arctic Alaska against the rigid North American craton (Estève et al., 2022). The RM, located at the edge of the craton, acted as a buttress that focused the escape and northward deformation of supra-crustal rocks into the Beaufort Sea (Lane, 1998; Estève et al., 2022).

The Porcupine fault system (PFS), located west of the RM, is a major northeast-striking fault zone that forms the southeastern boundary of the Arctic Alaska terrane (Colpron et al., 2019; Faehnrich et al., 2025). The PFS has recorded polyphase brittle–ductile deformation, including evidence of older sinistral displacement and younger dextral brittle movement (von Gosen et al., 2019). New geochronological data constrain Mesozoic deformation within the PFS to about 121 Ma (U-Pb dating of calcite veins), supporting translational or hybrid models for the opening of the Canada Basin that involved significant strike-slip motion of the Arctic Alaska terrane (McClelland et al., 2021; Faehnrich et al., 2025). The complex, contrasting kinematics observed in the RFS and PFS underscore the distributed nature of strain partitioning necessary to accommodate the convergence and rotations of crustal blocks within the northwestern Cordillera.

Seismicity

The RM region is one of the most seismically active zones along the eastern Cordillera mountain front in northwest Canada (Cassidy et al., 2005; Hyndman et al., 2005a; Hyndman et al., 2005b). This activity is proposed to be the result of far-field strain transfer originating from the oblique collision of the Yakutat terrane in the Gulf of Alaska, pushing the northern Cordilleran block northeastward (Mazzotti and Hyndman, 2002; Hyndman et al., 2005; Leonard et al., 2007). This rigid displacement of the upper crust, estimated at approximately 5 ± 4 mm/year relative to the stable North American craton, is accommodated in the RM primarily by strike-slip motion (Mazzotti and Hyndman, 2002; Leonard et al., 2007; Mazzotti et al., 2008; Rohr et al., 2011). An alternative driving mechanism for enigmatic Cenozoic deformation along the eastern margin of the NCC is rooted far from the active Pacific margin. Enkelmann et al. (2019) hypothesize that Early Oligocene deformation (~40–30 Ma) recorded through renewed exhumation in the RM is potentially related to stresses originating from the eastern boundary of the North American plate, located approximately 4000 km away. Specifically, this model links episodes of deformation and exhumation in the NCC to changes in the absolute plate motion of

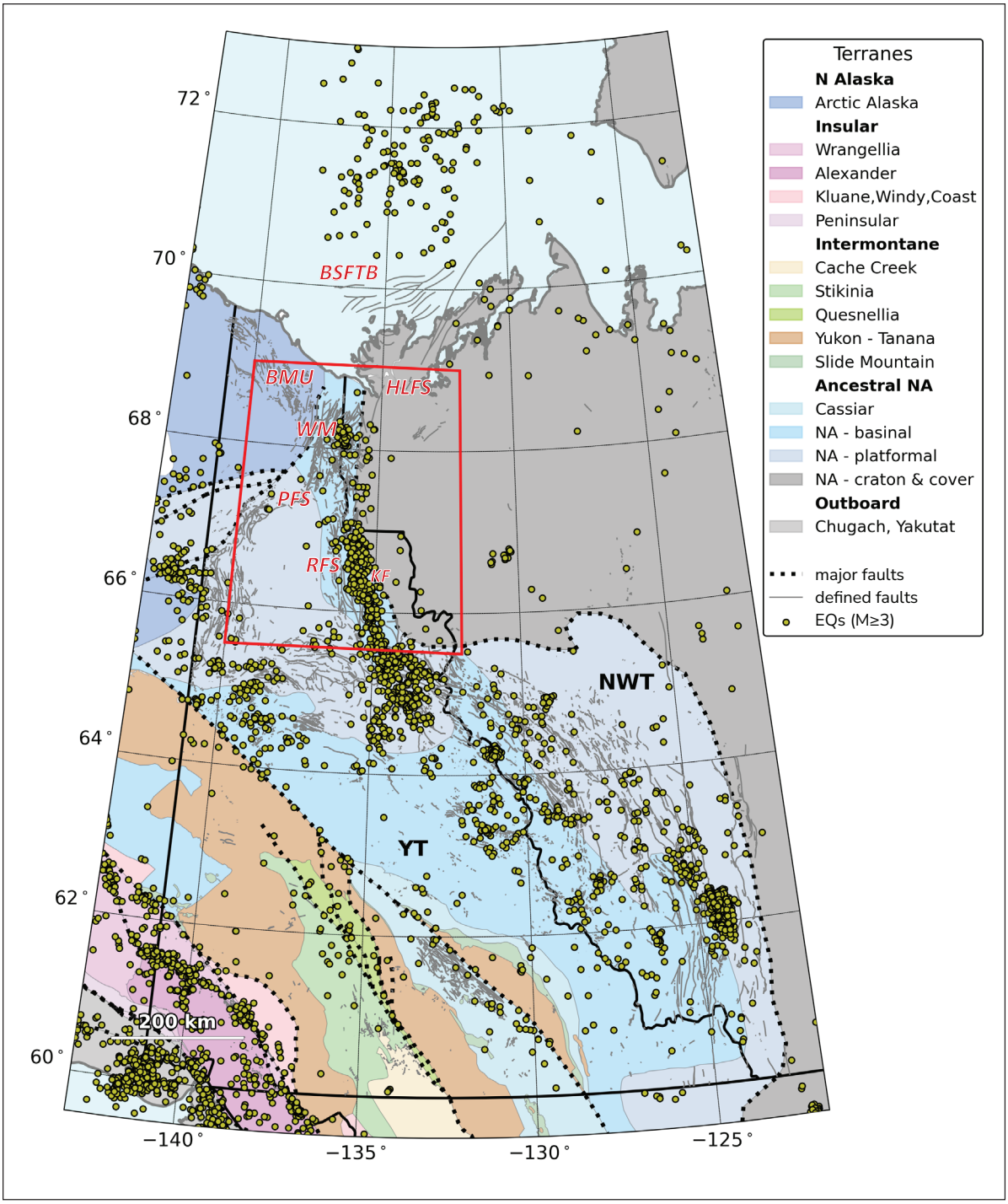

Figure 1. *Map of the Yukon and the westernmost region of the Northwest Territories. Terranes are taken from Nelson et al. (2013), and major faults are dashed lines and light grey lines denoting 'defined' faults extracted from the databases of the Yukon and Northwest Territories geological surveys (Yukon Geological Survey, 2016; Northwest Territories Geological Survey, 2018). Yellow circles denote the locations of earthquakes with M≥3.0. The red square denotes the Richardson Mountains study region illustrated in subsequent Figures 2 and 3. Labels denote regions discussed in the main text: BMU: Barn Mountains uplift; BSFTB: Beaufort Sea fold and hrust belt; HLFS: Husky Lakes fault system; KF: Knorr fault; PFS: Porcupine fault system; RFS: Richardson fault system; WM: White Mountain uplift.*

North America, particularly during periods when the plate's velocity increased and its motion was oriented at a high angle to the pre-existing structural grain of the Cordillera. This suggests that the opening of the North Atlantic Ocean provided the necessary far-field tectonic forcing (Enkelmann et al., 2019; Stephan and Enkelmann, 2025).

The RM remain seismically active today (Cassidy and Bent, 1993; Pinet, 2021), and seismicity is concentrated along the RFS, a system of steep north-south trending faults that extend northward toward the Beaufort Sea (Cassidy and Bent, 1993; Mazzotti and Hyndman, 2002; Hyndman et al., 2005; Pinet, 2021). The largest recorded earthquakes in this region occurred in close succession in 1940: M_S = 6.2 on May 29, and M_S = 6.5 on June 5 (Cassidy and Bent, 1993; Hyndman et al., 2005a; Hyndman et al., 2005b). These major events were complex ruptures, with focal depths ranging from 14.5 to 11 km for the May event, and 10 to 7 km for the June event, generally located in the mid to upper crust (Cassidy and Bent, 1993; Hyndman et al., 2005a; Hyndman et al., 2005b). In general, earthquakes in the RM are characterized by right-lateral strike-slip motion along the north-south trending planes (Cassidy and Bent, 1993; Cassidy et al., 2005). Structural analysis of the RFS shows that this dextral movement often affects previously tilted and deformed sedimentary successions, highlighting a history of polyphase deformation (Pinet, 2021). The orientation of the pressure axes for these earthquakes is northeast-southwest, consistent with the contemporary regional stress field that influences the entire northern Cordillera (Cassidy and Bent, 1993; Hyndman et al., 2005; Gosselin et al., 2024).

Focal mechanism studies, including analysis of 1940 events and subsequent moderate earthquakes (M_b = 4.8 in 1972 and M_b = 5.0 in 1976), consistently show a dominant right-lateral strike-slip faulting motion along the Richardson Mountains fault system (Cassidy and Bent, 1993; Cassidy et al., 2005; Hyndman et al., 2005b; Leonard et al., 2007; Pinet, 2021). For the 1940 events, the preferred interpretation is the right-lateral motion along north-south trending planes, consistent with mapped surface faults in the region (Cassidy and Bent, 1993). The pressure axes (maximum horizontal stress) determined from these focal mechanisms are oriented northeast-southwest (~N40°E), indicating that the contemporary regional stress field is reactivating the pre-existing, favourably oriented faults of the RFS (Cassidy and Bent, 1993; Mazzotti and Hyndman, 2002; Hyndman et al., 2005a; Hyndman, et al., 2005b). This compressional orientation is similar to that found in the northern Mackenzie Mountains, suggesting that both regions are driven by the same far-field stress, although the Mackenzie Mountains predominantly exhibit thrust faulting (Cassidy and Bent, 1993, 2025; Hyndman et al., 2005b).

A key feature of the seismicity is the lack of aftershocks for the 1940 Richardson Mountains earthquakes, which is consistent with the estimated low stress drops of 22 to 28 bars for these events, similar to other major earthquakes in the eastern Canadian Cordillera (Cassidy and Bent, 1993, 2025). The largest earthquakes in the region occur frequently in pairs or swarms, suggesting that stress triggering plays an important role (Cassidy and Bent, 1993, 2025; Cassidy et al., 2005). The RM represent a high seismic hazard zone, with an estimated return period for a potentially damaging earthquake (M≥5) of about 2–3 years (Cassidy et al., 2005; Hyndman et al., 2005). Based on the maximum geological and seismic extent of the main strike-slip fault system (estimated at 200 km), the maximum possible magnitude is estimated to be M_x = 7.5 (ranging from 7.2–7.8; Mazzotti and Hyndman, 2002; Hyndman et al., 2005a; Hyndman et al., 2005b). Despite the importance of the Richardson Mountains as a kinematic pivot point, the locus of current displacement and magnitude along the RFS is poorly constrained (Pinet, 2021).

Data and methods

Earthquake catalogues

The source of events used in this study is Canada's National Earthquake Database (NEDB; Canadian Hazards Information Service, 1985), originally created and curated by the Geological Survey of Canada (GSC), and now by the Canadian Hazards Information Service (CHIS) within Natural Resources Canada (NRCan). This database is the long-term primary national database for seismicity within and near Canada, and is used as the source of earthquake information for the Canadian National Seismic Hazard Model (CNSHM; Kolaj et al., 2023). Events within this catalogue have been located and reviewed by analysts since its inception, and historical earthquake epicentres were added through the archival study of reports of ground shaking and damage dating back hundreds of years. The 'modern' catalogue originated in 1985 when seismic data increased in availability.

In Figures 1 and 2 we plot events from the NEDB that have occurred since 1985, located within the study

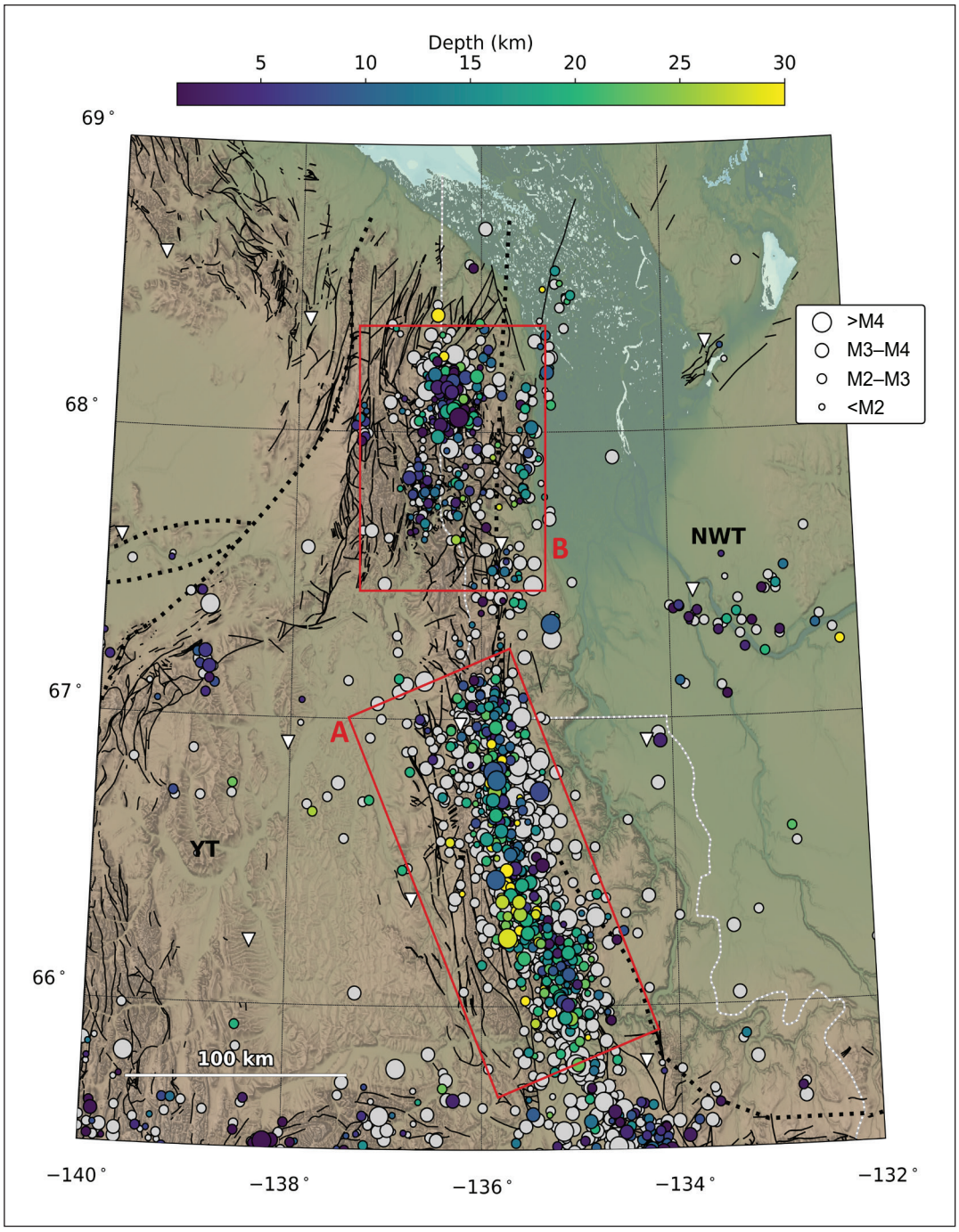

Figure 2. *Map of earthquakes extracted from the Canadian Hazards Information Service (CHIS) National Earthquake Database (NEDB; Canadian Hazards Information Service, 1985) for the region of interest. Earthquake magnitudes are indicated by the size of the circle, and the colour of the circle denotes the earthquake depth. The events coloured by depth are those events that occurred within the period for the relocation, from January 1, 2015 to December 31, 2021. The light grey circles denote the rest of the events in the NEDB, outside this time period. Inverted white triangles denote the location of operating seismic stations during this time period. Regions A and B are indicated by red boxes, as discussed in text.*

region. In Figure 1 only events M≥3.0 are illustrated to highlight seismically active areas in the broader regional context. In Figure 2, which focuses on our study region of the RM, we include all events in the NEDB sized according to event magnitude. Events for the time period between 2015 and 2021 are coloured according to depth and are used as input to the analysis in this work. Events indicated in grey are all remaining NEDB events outside this time period to illustrate the spatial distribution of events in the entire catalogue. Within the confines of the RM study region in Figure 2, there are a total of 1595 events in the NEDB, including 775 within the selected 2015 to 2021 period.

The distribution of these events is clearly concentrated in two regions associated with the RFS: the southern main strand between 66.5°N and 67.25°N (region A, Figs. 2 and 3), and a northern cluster centred around 68°N (region B, Figs. 2 and 3). The depths of seismicity within this region are poorly constrained between the surface and ~40 km depth. Some diffuse additional seismicity is observed off-axis of the RFS, potentially accommodating stress release on more localized structures to the west or reflecting uncertainties in event locations. Limited diffuse seismicity is also observed to the east, within the Mackenzie Delta region.

For this analysis, we extracted events in the period extending from January 1, 2015 to December 31, 2021 from the NEDB. This range is selected because it corresponds to the highest density of seismic station coverage in the area, due to the deployment of the USArray Transportable Array (TA; IRIS Transportable Array, 2003; Busby and Aderhold, 2020), in Alaska, Yukon, and the westernmost region of the Northwest Territories. The improved station coverage during this period enabled a significant reduction in the detection threshold and magnitude of completeness of the earthquake catalogue, resulting in significantly more recorded events (Ruppert and West, 2020). Although most of the TA stations were removed during 2021, a select number of these were retained by the GSC (PQ; Geological Survey of Canada, 2013) and CHIS (CN; Natural Resources Canada, 1975). Some of these adopted stations have contributed to the ongoing work of the Western Arctic Regional Network of Seismographs (WARNS; Schaeffer et al., 2025).

Double-difference relocation

We used the double-difference (DD) relocation method in order to better constrain the seismicity patterns throughout the RM region. The DD relocation method is a widely used seismological technique designed to improve relative earthquake hypocentres, and includes many successful applications. In many cases, the absolute location of events is also improved (Biegel et al., 2024b). Improved relative locations can illuminate active fault systems, allowing improved interpretation and understanding of geological processes. This methodology, typically implemented in software such as *HypoDD* (Waldhauser, 2001) or its advanced variants, leverages the additional information available when considering multiple events jointly, rather than independently located individual earthquakes.

The DD method is fundamentally a relative location technique that treats the estimation of the locations of all events within a cluster of earthquakes as a single inverse problem. Rather than considering the observed data as absolute travel times, the data are considered differential travel times (Waldhauser and Ellsworth, 2000; Waldhauser, 2001). Specifically, the data are the differences in travel times for events (within the same cluster) recorded by the same stations. The goal of the DD approach is to minimize the residuals for these differential travel times (i.e., the differences between observed and predicted differential travel times). Hence, the objective function for this problem is defined as a difference of differences, which is where the term double-difference originates. The DD method ultimately minimizes spatial distance errors between neighbouring events, allowing more precise identification of geological structures, such as active fault planes, with high fidelity (Waldhauser and Ellsworth, 2000; Waldhauser, 2001).

A fundamental inherent advantage to the DD approach is that if two earthquakes occur in near proximity, the paths that the seismic waves travel along to a recording seismic station will be similar, particularly outside of the earthquake source region. By treating the data as the difference in arrival times for this event pair, any errors introduced by complex or unmodeled velocity structures along the propagation path to the station are minimized. This process, known as common mode error suppression, focuses location sensitivity primarily on the region near the source (Jordan and Sverdrup, 1981; Got et al., 1994; Waldhauser and Ellsworth, 2000). This avoids the need for explicit station correction terms typical in older relocation methods (Douglas 1967; Waldhauser and Ellsworth 2000).

By reducing velocity-model and station-correction errors, DD relocations typically improve location precision by orders of magnitude compared to

traditional catalogue locations (Waldhauser and Ellsworth, 2000; Waldhauser and Schaff, 2008). This transformation collapses diffuse seismicity clusters into sharply defined structures (Got et al., 1994; Schaff et al., 2002; Wolfe, 2002). For example, studies on the Northern Hayward fault showed that DD relocations collapsed diffuse locations into sharp images, revealing previously hidden structures such as horizontal lines of hypocentres (Waldhauser and Ellsworth, 2000). This increased resolution allows seismicity to be restricted to specific geological units, providing excellent depth constraints, particularly valuable in induced seismicity studies (Rubin et al., 1999; Biegel et al., 2024b). Similar methods applied in southern Yukon have illuminated a network of discrete faults, as well as previously unknown faults, that accommodate deformation due to oblique collision of the Yakutat microplate with North America (Biegel et al., 2022; Biegel et al., 2024a).

In this work, we apply the DD algorithm by integrating two types of data into the inverse problem. First, traditional arrival times for the P and S-wave phases are obtained from the original NEDB. These catalogue data constrain the larger relative locations between distant earthquake clusters (multiplets) and uncorrelated events (Douglas, 1967; Waldhauser and Schaff, 2008). Second, for events with similar seismic waveforms ('doublets' or 'multiplets'), waveform cross correlations are used to measure the differential arrival times with sub-millisecond precision. These waveform cross-correlation data can yield measurements with precision orders of magnitude higher than manual phase selection (Poupinet et al., 1984; Schaff et al., 2004). Combining DD relocation catalogue data with waveform cross-correlation data is widely considered the most effective way to produce high-resolution event locations, and determine inter-event distances within multiplets to the highest accuracy (Poupinet et al., 1984; Waldhauser and Ellsworth, 2000).

We applied the DD approach to the selection of 775 earthquakes extracted from the NEDB, as outlined in the previous section. In this analysis, we used both the catalogue phase data and the calculated waveform cross-correlation data, inverting these simultaneously using the *scrtdd* (Scarabello et al., 2025) implementation of *HypoDD* integrated into the SeisComP software environment (Helmholtz Centre Potsdam GFZ German Research Centre for Geosciences and gempa GmbH, 2008). All combinations of waveform pairs for these events are cross correlated, and the resulting differential travel times are inverted with the catalogue phase arrival times to produce the final DD relocated catalogue. In this relocation analysis, we use a 1D reference model calculated from a regional average of the velocity model derived by Estève et al. (2022). For the DD relocation, we performed a number of iterations to explore the results based on selectable parameters in the software, and used the parameterizations below:

- a minimum of 4 defining phases common between stations;
- a minimum of 4 neighbouring events for each event in a chain;
- a maximum of 80 neighbouring events for each event in a chain;
- a maximum search ellipsoid of 10 km;
- P-wave minimum cross-correlation coefficient of 0.5;
- P-wave cross-correlation window of ± 0.75 s around the phase arrival;
- S-wave minimum cross-correlation coefficient of 0.5;
- S-wave cross-correlation window of ± 1.0 s around the phase arrival;
- waveforms band-pass filtered between 1–20 Hz;
- minimum signal to noise ration (SNR) of 2 for phases;
- noise window -3 s to -0.35 s prior to the phase arrival; and
- signal window -0.35 s to 1.0 s around the phase arrival.

Many of the selected parameters optimum values are dictated by the relative geometry of the stations and the events in the region (i.e., the distances between pairs of events and stations).

Results and discussion

Figure 3 illustrates our relocated earthquake catalogue for the RM region. It is apparent from examining the catalogue in map view that the quality control steps inherent to the DD workflow has removed some isolated seismicity (i.e., not in spatial clusters) that occurred throughout the region. It is important to note that this does not suggest that these events are not

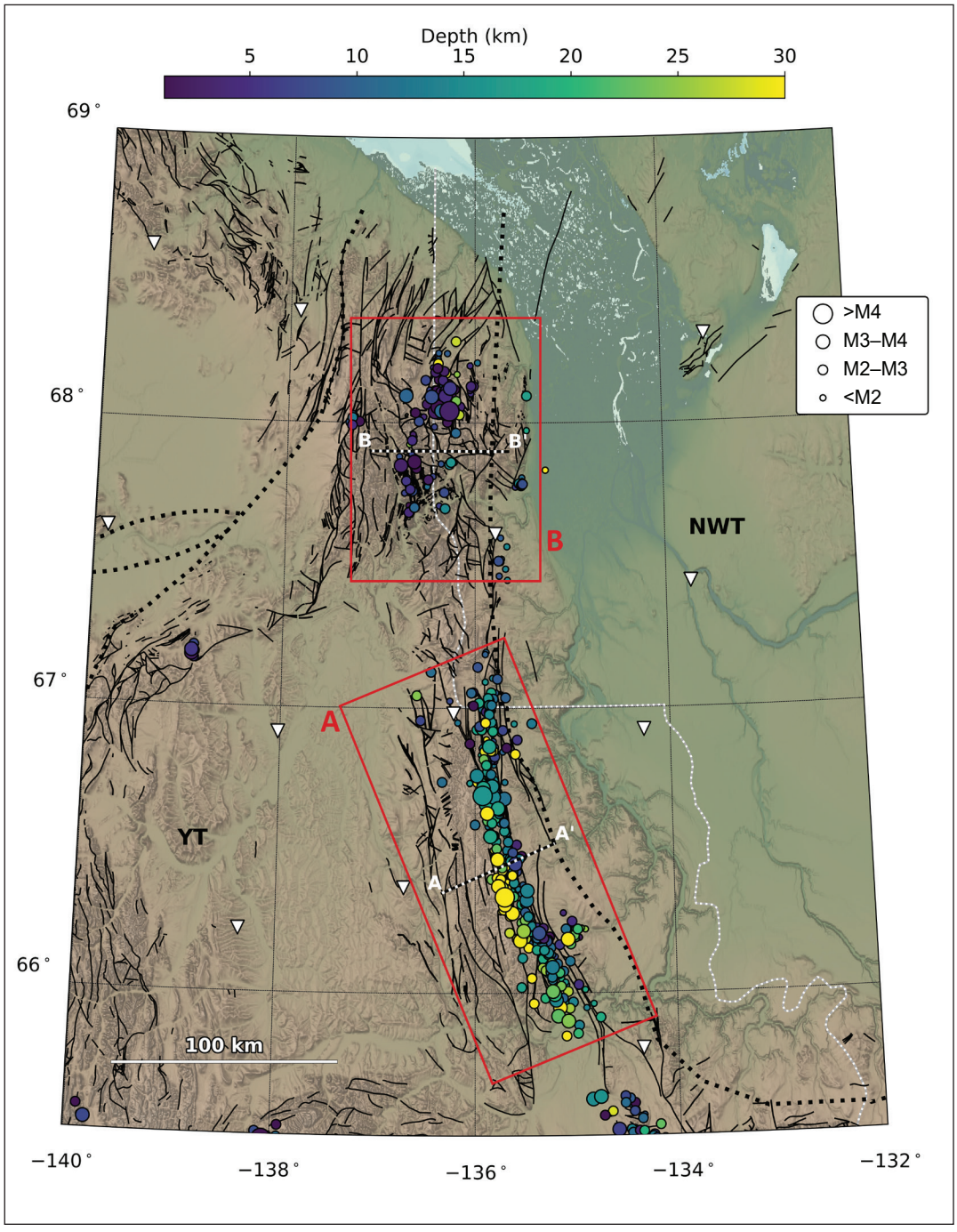

Figure 3. *Map view of the relocated catalogue of 594 earthquakes across the Richardson Mountains study region. Earthquake depths are denoted by the colour of the circle, and magnitudes by the size of the circle. Major faults are plotted as dotted lines and 'defined' faults as solid lines, from the Yukon Geological Survey (Yukon Geological Survey, 2016) and Northwest Territories Geological Survey (Northwest Territories Geological Survey, 2018) online repositories. Regions A and B are indicated by red boxes, as discussed in text. Two cross-sectional profiles, A–A' and B–B', are indicated by dashed lines, and illustrated in Figure 5.*

real, or that there is no seismicity where the events have been removed. Rather, this simply indicates that there is not sufficient seismicity to be robustly inverted within the DD framework. Therefore, the isolated events are excluded from our subsequent analysis. The final relocated catalogue includes 594 events.

The relocated earthquake catalogue highlights three main areas where seismicity meets the DD criteria for clustering, and as a result the spatial patterns of these events are much more clearly illuminated. The first area is the seismicity at the southernmost extent of the map, at the corner where the RM rotate and meet the Mackenzie Mountains. Second, moving northward, the most significant cluster of seismicity is associated with the main strand of the RFS, and locates predominantly along the easternmost front range of the RM, between approximately 65.75°N and 67.25°N. We refer to this region as A and denote the cross-section through it with profile A–A'. Finally, there is a more distributed zone of seismicity farther to the north, which we refer to as B, and illustrate with the cross-section profile B–B'. Region B seismicity occurs immediately to the north of the Richardson anticlinorium, within the White Mountains uplift of the Babbage basin (see Figure 2, Cecile et al., 2022). We observe a paucity of seismicity along the RM in the area between the main regions of seismicity A and B. We note that this lack of seismicity is also apparent in the original NEDB and is likely not due to the DD clustering and quality control processes. This may indicate that either regions A and B are distinct and disconnected, or that this intervening zone is presently locked.

Figure 4 illustrates the depth distributions of events in the NEDB catalogue and the relocated DD catalogue. The peaks in depth values for the NEDB are a result of fixing the depths manually by seismic analysts for most events when there were insufficient stations to constrain a free depth during the original location process. Different values of the fixed depth have been used over decades of the catalogue, resulting in the artificial peaks observed at 1, 5, 10, 15 and 20 km depths. In the relocated DD catalogue, it is clear that the depth distribution of events has been reallocated across the range; however, 2/3 to 3/4 of events are located to

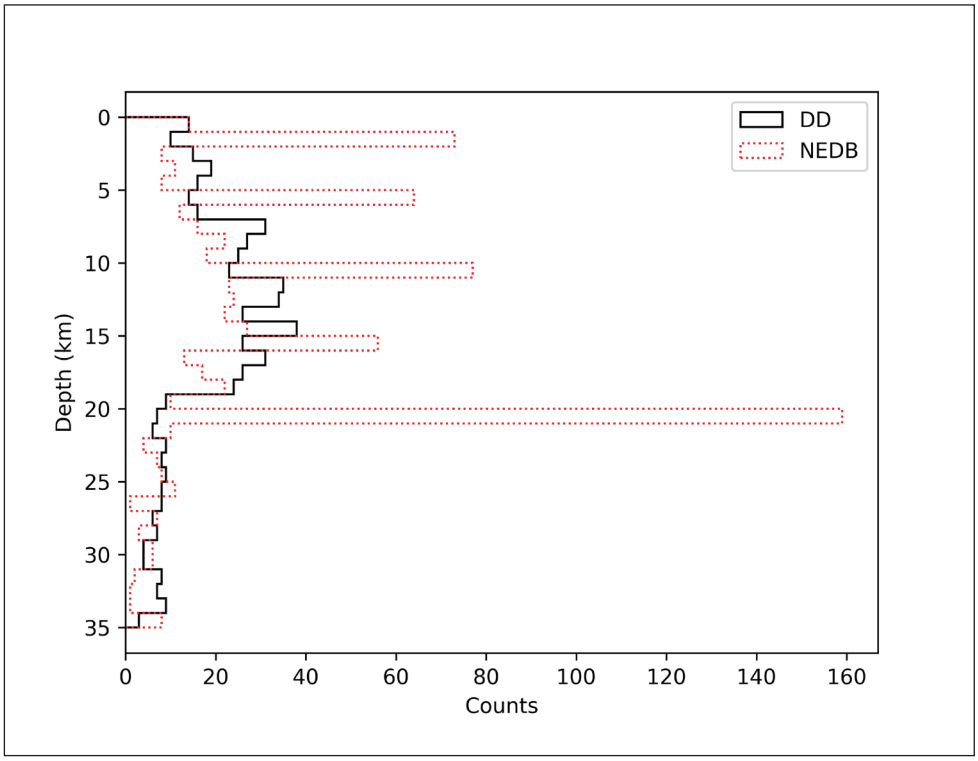

Figure 4. *Histograms of earthquake depths computed for the NEDB events (in red) within the Richardson Mountains study region and the relocated double-difference (DD) catalogue (in black). We note that the peaks in the depths of the NEDB depth distribution are due to common fixed event depths when free depths could not be constrained. These artifacts are removed by the DD relocation process.*

depths shallower than 20 km. Figure 5 illustrates the depths of seismicity along the profiles A–A' and B–B'. The profile locations are shown in Figure 3. All events within 20 km of the profile are projected onto it. The figure further highlights the catalogue artifacts due to manual selection of event depths in the NEDB, as well as the general diffusivity of seismicity.

Region A

Upon examination of region A in Figures 2 and 3, it is clear that the relocation procedure has significantly reduced the diffusivity of the pattern of seismicity, and events are concentrated along the easternmost edge of the RFS. Most of these events locate inboard of the inferred eastern limit of Cordilleran deformation (the dashed black line east of region A seismicity in Figure 3). Furthermore, the main branch of seismicity appears to align along a sub-linear feature dipping westward. The dip of this cluster of seismicity is clearly seen in cross-sectional view (Figure 5), and events at the eastern leading edge are shallower and deepen westward.

Figure 5a,c illustrates the vertical extent of seismicity for profile A–A'. The top panel (Fig. 5a) illustrates the NEDB catalogue along this profile: the grey circles are the complete NEDB, whereas those in red represent the window from 2015 to 2021 during the TA deployment and improved seismic station density. It is challenging to identify any consistent spatial pattern in the precise east–west concentration of seismicity, nor any specific pattern in depth, when considering the entire

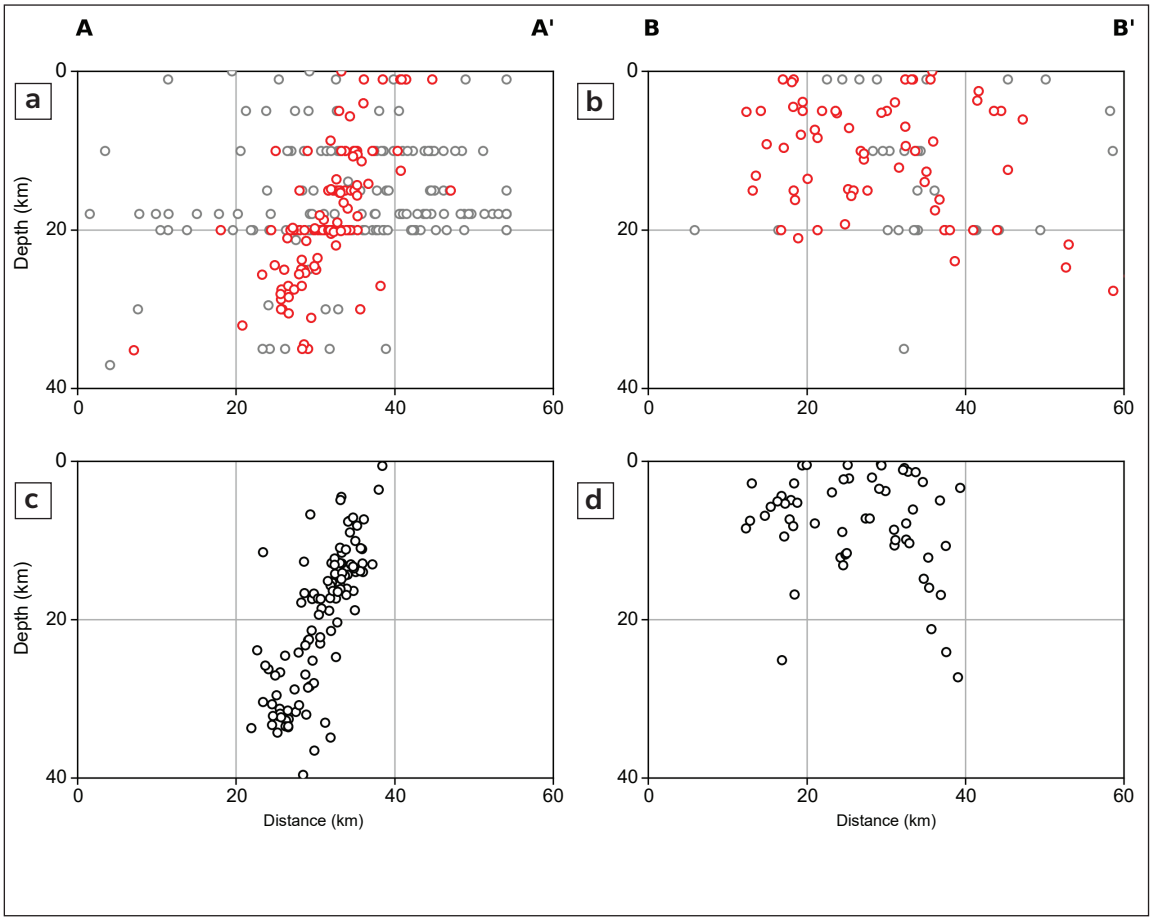

Figure 5. *Cross-sections of earthquake catalogues. Seismicity in the NEDB is displayed in plots* **(a)** *and* **(b)**. *Events considered for relocation are illustrated in red, other NEDB events (mostly outside of the 2015 to 2021 period) are illustrated in grey. Seismicity in the relocated catalogue is illustrated in plots* **(c)** *and* **(d)**. *Locations of cross sections (A–A' and B–B') are illustrated in Figure 3.*

NEDB. However, the relocated DD catalogue along A–A' (Fig. 5c), defines a clear, consistent westward-dipping structure, from near the surface to a depth of ~35 km, which is the inferred base of the crust (Audet et al., 2020). Based on the width of the seismicity across this depth range, we estimate the dip of this seismogenic zone to be ~75°. Both the depth and the dip of this seismogenic zone are consistent across the 150 km north–south extent. Notably, this seismicity is significantly deeper than observed in other parts of the Yukon (Drooff and Freymueller, 2023; Biegel et al., 2024a), highlighting the unique deformation in the RM area.

Extrapolating this dipping feature to the surface along most of its north–south length, it appears to intersect very closely with the surface trace of the easternmost segments of the Knorr fault, a normal fault that accommodated past rifting (e.g., Cecile et al., 1985; Cecile et al., 2022). The direction and dip of the seismogenic zoom we observe is compatible with modern seismicity reactivating an existing normal structure at depth.

Region B

Farther to the north, the seismicity of region B is not narrowly concentrated along the eastern front ranges of the RM, as is the case with seismicity in region A. Instead, here, we observe diffuse seismicity across the mountain range, despite the DD relocations. We note that the topographic expression is much wider in this region, as it incorporates a wider zone of deformation encompassing the White Mountains uplift, Barn uplift, and stretching to the British Mountains farther west. Along the southern boundary of this region, the PFS enters from the southwest, whereas the RFS enters from the south at the southeast corner. Finally, the HLFS departs to the northeast from the northernmost extent of the front ranges. This zone therefore records a complex interplay of pre-existing structures that supported significant amounts of deformation over hundreds of millions of years . In this context, the more distributed seismicity occurring across this region, suggests there is no single preferred active fault strand on which the seismicity has coalesced, in contrast to region A. Rather, seismicity clearly remains distributed across much of the width of the mountain range and active deformation zone.

The distribution of seismicity indicated in cross-section B–B' is illustrated in Figure 5b,d. Here, the differences between the starting NEDB catalogue and the relocated catalogue appear laterally less significant compared to region A. The apparent loss of seismicity east of the 40 km point along the profile is predominantly due to the clustering and quality control processes. The relatively sparse seismicity along the Bug Creek fault, the presumed active easternmost fault of the Aklavik Front Ranges, is retained as a consequence of selecting only those events suitable for inversion of differential travel times. However, we note that the relocation procedure indicates that much of the seismicity in region B is hosted on shallow (<10 km deep) structures, or that the seismogenic thickness of the crust in this area is more limited (Biegel et al., 2024a). This is consistent with previous observations of Estève et al. (2022), who propose the seismogenic thickness of the crust shallows northward through the RM, potentially due to increasing crustal temperatures.

Concluding remarks

This work re-examines a subset of the modern earthquake catalogue in northwestern Canada, along the RM, through application of the DD earthquake relocation process. Our relocated catalogue leads to several key findings, listed below.

- There is a reliability of inferred earthquake depths with the removal of catalogue artifacts due to manually fixed depths in the 0–20 km range.

- Much of the seismicity along the main branch of the RM is in close proximity to the surface expression of the Knorr fault and maintains a consistent ~75° westward dip along the entire ~150 km length of the easternmost edge of the RFS. This is compatible with reactivation of the normal fault surface of the Knorr fault.

- Seismicity farther north along the RM, within the complex White Mountains and Barn uplifts, is more diffuse without a dominant active structure.

These preliminary findings motivate the need for ongoing and additional study of active tectonics in the area. Specifically, the utilization of additional data recorded on seismic stations deployed recently through the WARNS initiative will enable further enhancement of earthquake catalogues. An outstanding tectonic question is the connection and relation of the Bug Creek fault to the HLFS. Additionally, the seismic quiescence along a ~75 km segment of the RM that we note from

both the NEDB and our relocated catalogue may imply a seismic gap or a change in seismogenic capacity of the crustal column. This has implications for maximum possible seismogenic fault size, and therefore seismic hazards. These questions will be addressed in future work. Our initial re-examination of the modern earthquake catalogue in the RM will contribute to improved understanding of the geological history and resource potential of the region, as well as support decision-making that mitigates natural hazards for Canada's northern communities.

Competing interests

The authors of this manuscript declare no competing interests.

Acknowledgments

We respectfully acknowledge and thank Yukon First Nations and Alaska Natives for providing access to their lands to install most of the seismic instruments used in this study. We are grateful to reviews from C. Estève (University of Vienna). Seismic data used in this study was obtained from the Earthscope Data Management Centre and the Canadian Hazards Information Service National Data Repository.

References

Audet, P., Schutt, D.L., Schaeffer, A.J., Estève, C., Aster, R.C. and Cubley, J.F., 2020. Moho variations across the northern Canadian Cordillera. Seismological Society of America, vol. 91, no. 6, p. 3076–3085.

Biegel, K., Gosselin, J.M. and Dettmer, J., 2022. Preliminary double-difference relocation earthquake catalogue for southwestern Yukon centred along the Denali fault zone. *In:* Yukon Exploration and Geology 2022, K.E. MacFarlane (ed.), Yukon Geological Survey, Government of Yukon, p. 1–18, plus digital appendices.

Biegel, K., Gosselin, J.M., Dettmer, J., Colpron, M., Enkelmann, E. and Caine, J.S., 2024a. Earthquake relocations delineate a discrete fault network and deformation corridor throughout southeast Alaska and southwest Yukon. Tectonics, vol. 43, no. 5, https://doi.org/10.1029/2023TC008140.

Biegel, K.M., Dettmer, J., Igonin, N. and Eaton, D.W., 2024b. Double-pair double-difference relocation improves depth precision and highlights detailed 3D fault geometry for induced seismicity in Alberta, Canada. Seismological Research Letters, vol. 96, no. 3, p. 100–112, https://doi.org/10.1785/0220240194.

Busby, R.W. and Aderhold, K., 2020. The Alaska transportable Array: As built. Seismological Research Letters, vol. 91, no. 6, p. 3017–3027, https://doi.org/10.1785/0220200154.

Canadian Hazards Information Service, 1985. Canadian National Earthquake Database. Natural Resources Canada, https://doi.org/10.17616/R3TD24 [accessed 15/11/2025].

Cassidy, J.F. and Bent, A.L., 1993. Source parameters of the 29 May and 5 June, 1940 Richardson Mountains, Yukon Territory, earthquakes. Bulletin of the Seismological Society of America, vol. 83, no. 3, p. 636–659, https://doi.org/10.1785/BSSA0830030636.

Cassidy, J.F. and Bent, A.L., 2025. The Mackenzie Mountains, Northwest Territories, earthquake sequence of 1953 to 1957. Canadian Journal of Earth Sciences, vol. 62, no. 4, p. 923–937, https://doi.org/10.1139/cjes-2024-0132.

Cassidy, J.F., Rogers, G.C. and Ristau, J., 2005. Seismicity in the vicinity of the Snorcle corridors of the northern Canadian Cordillera. Canadian Journal of Earth Sciences, vol. 42, no. 6, p. 1137–1148.

Cecile, M., Hutcheon, I.E. and Gardner, D., 1985. Geology of the northern Richardson anticlinorum. Geological Survey of Canada, Open File 875.

Cecile, M.P., Morrow, D.W. and Williams, G.K., 1997. Early Paleozoic (Cambrian to Early Devonian) tectonic framework, Canadian Cordillera. Bulletin of Canadian Petroleum Geology, vol. 45, no. 1, p. 54–74.

Cecile, M.P., Norford, B.S., Nowlan, G.S. and Uyeno, T.T., 2022. Lower Paleozoic stratigraphy and geology, Richardson Mountains, Yukon (with stratigraphic and paleontological appendices). Geological Survey of Canada, Bulletin 614, https://doi.org/10.4095/329454.

Colpron, M., Strauss, J.V. and McClelland, W.C., 2019. Detrital zircon U-Pb geochronological and Hf isotopic constraints on the geological evolution of North Yukon. *In:* Circum-Arctic Structural Events: Tectonic Evolution of the Arctic Margins and Trans-Arctic Links with Adjacent Orogens, K. Piepjohn, J.V. Strauss, L. Reinhardt and W.C. McClelland (eds.), Geological Society of America Special Paper, Geological Society of America, vol. 541, p. 397–437, https://doi.org/10.1130/2018.2541(19).

Douglas, A., 1967. Joint epicentre determination. Nature, vol. 215, p. 47–48.

Drooff, C. and Freymueller, J.T., 2023. New insights into the active tectonics of the northern Canadian Cordillera from an enhanced earthquake catalog. Journal of Geophysical Research: Solid Earth, vol. 128, no. 12, https://doi.org/10.1029/2023JB026793.

Enkelmann, E., Finzel, E. and Arkle, J., 2019. Deformation at the eastern margin of the northern Canadian Cordillera: Potentially related to the opening of the North Atlantic. Terra Nova, vol. 31, no. 3, p. 151–158, https://doi.org/10.1111/ter.12374.

Estève, C., Liu, Y., Koulakov, I., Schaeffer, A.J. and Audet, P., 2022. Seismic evidence for a weakened thick crust at the Beaufort Sea continental margin. Geophysical Research Letters, vol. 49, https://doi.org/10.1029/2022GL100158.

Eyster, A.E., Fu, R.R., Strauss, J.V., Weiss, B.P., Roots, C.F., Halverson, G.P., Evans, D.A.D. and Macdonald, F.A., 2017. Paleomagnetic evidence for a large rotation of the Yukon block relative to Laurentia: Implications for a low-latitude Sturtian glaciation and the breakup of Rodinia. Geological Society of America Bulletin, vol. 129, no. 1/2, p. 38–58.

Faehnrich, K., McClelland, W.C., Webb, L.E., Rasbury, E.T., Colpron, M. and Strauss, J.V., 2025. Cretaceous strike–slip displacement along the Porcupine fault system and potential links to the opening of the Canada Basin. Canadian Journal of Earth Sciences, vol 62, no. 10, https://doi.org/10.1139/cjes-2025-0013.

Gabrielse, H., 1991. Structural Styles. *In:* Geology of the Cordilleran Orogen in Canada, H. Gabrielse and C.J. Yorath (eds.), Geology of Canada, Geological Survey of Canada, p. 571–675.

Geological Survey of Canada, 2013. Public Safety Geoscience Program Canadian Research Network. International Federation of Digital Seismograph Networks. https://doi.org/10.7914/SN/PQ [accessed 30/11/2025].

Gosselin, J.M., Biegel, K.M., Dettmer, J., Gilbert, H., Colpron, M. and Enkelmann, E., 2024. Crustal stress near the Yakutat microplate collision from probabilistic earthquake focal mechanisms. Canadian Journal of Earth Sciences, vol. 62, no. 4, p. 807–820, https://doi.org/10.1139/cjes-2024-0095.

Got, J.-L., Fréchet, J. and Klein, F.W., 1994. Deep fault plane geometry inferred from multiplet relative relocation beneath the south flank of Kilauea. Journal of Geophysical Research, vol. 99, no. B8, p. 15375–15386.

Helmholtz Centre Potsdam GFZ German Research Centre for Geosciences and gempa GmbH, 2008. The SeisComP seismological software package, GFZ Data Services, https://doi.org/10.5880/GFZ.2.4.2020.003.

Hyndman, R.D., Cassidy, J.F., Adams, J., Rogers, G.C. and Mazzotti, S., 2005a. Earthquakes and seismic hazard in the Yukon-Beaufort Mackenzie. Canadian Society of Exploration Geophysicists, Recorder, vol. 30, no. 5, p. 32–43.

Hyndman, R.D., Flück, P., Mazzotti, S., Lewis, T.J., Ristau, J. and Leonard, L., 2005. Current tectonics of the northern Canadian Cordillera. Canadian Journal of Earth Sciences, vol. 42, no. 6, p. 1117–1136, https://doi.org/10.1139/e05-023.

IRIS Transportable Array, 2003. USArray Transportable Array. International Federation of Digital Seismograph Networks, https://doi.org/10.7914/SN/TA [accessed 30/11/2025].

Jeletsky, J.A., 1962. Pre-Cretaceous Richardson Mountains trough—Its place in the tectonic framework of Arctic Canada and its bearing on some geosynclinals concepts. Transactions of the Royal Society of Canada, vol. 56, no. 3, p. 55–84.

Jordan, T.H. and Sverdrup, K.A., 1981. Teleseismic location techniques and their application to earthquake clusters in the South-Central Pacific. Bulletin of the Seismological Society of America, vol. 71, no. 4, p. 1105–1130.

Kolaj, M., Halhcuk, S.C. and Adams, J., 2023. Sixth-generation seismic hazard model of Canada: Grid values of mean hazard to be used with the 2020 National Building Code of Canada (ver. 1.0). Geological Survey of Canada, Natural Resources Canada, Open File 8950, https://doi.org/10.4095/331497.

Lane, L.S., 1996. Geometry and tectonics of early Tertiary triangle zones, northeastern Eagle Plains, Yukon Territory. Bulletin of Canadian Petroleum Geology, vol. 44, p. 337–348.

Lane, L.S., 1997. Cretaceous and Tertiary. *In:* The Geology, Mineral and Hydrocarbon Potential of Northern Yukon Territory and Northwestern District of Mackenzie, D.K. Norris (ed.), Geological Survey of Canada, Natural Resources Canada, Bulletin 422, p. 301–318.

Lane, L.S., 1998. Late Cretaceous–Tertiary tectonic evolution of northern Yukon and adjacent Arctic Alaska. American Association of Petroleum Geologists Bulletin, vol. 82, no. 7, p. 1353–1371.

Lane, L.S., 2002. Tectonic evolution of the Canadian Beaufort Sea – Mackenzie Delta region: a brief review. Canadian Society of Exploration Geophysicists, Recorder, vol. 27, no. 2, p. 49–56.

Lane, L.S., 2007. Devonian–Carboniferous paleogeography and orogensis, northern Yukon and adjacent Arctic Alaska. Canadian Journal of Earth Sciences, vol. 44, no. 5, p. 679–694.

Lane, L.S. and Dietrich, J.R., 1995. Bedrock geology and offshore structural trends. *In:* Geological Atlas of the Beaufort-Mackenzie Area, J. Dixon (ed.), Geological Survey of Canada.

Leonard, L.J., Hyndman, R.D., Mazzotti, S., Nykolaishen, L., Schmidt, M. and Hippchen, S., 2007. Current deformation in the northern Canadian Cordillera inferred from GPS measurements. Journal of Geophysical Research, vol. 112, no. 11, p. 1–15, https://doi.org/10.1029/2007JB005061.

Mazzotti, S. and Hyndman, R.D., 2002. Yakutat collision and strain transfer across the northern Canadian Cordillera. Geology, vol. 30, no. 6, p. 495–498, https://doi.org/10.1130/0091-7613(2002)030<0495:YCASTA>2.0.CO;2.

Mazzotti, S., Leonard, L.J., Hyndman, R.D. and Cassidy, J.F., 2008. Tectonics, dynamics, and seismic hazard in the Canada–Alaska Cordillera. *In:* Active Tectonics and Seismic Potential of Alaska, J.T. Freymueller, P.J. Haeussler, R.L. Wesson and G. Ekström (eds.), vol 179, p. 297–319. AGU Geophysical Monograph Series, American Geophysical Union, https://doi.org/10.1029/179GM17.

McClelland, W.C., Strauss, J.V., Colpron, M., Gilotti, J.A., Faehnrich, K., Malone, S.J., Gehrels, G.E., Macdonald, F.A. and Oldow, J.S., 2021. Taters versus sliders: Evidence for a long-lived history of strike-slip displacement along the Canadian Arctic transform system (CATS). GSA Today, vol. 31, no. 7, p. 4–11, https://doi.org/10.1130/GSATG500A.1.

Morrow, D.W., 1999. Lower Paleozoic stratigraphy of northern Yukon Territory and northwestern District of Mackenzie. Geological Survey of Canada, Bulletin 538, 202 p., https://doi. org/10.4095/210998.

Natural Resources Canada, 1975. Canadian National Seismograph Network. Natural Resources Canada, https://doi.org/10.7914/SN/CN [accessed 30/11/2025].

Nelson, J.L., Colpron, M. and Israel, S., 2013. The Cordillera of British Columbia, Yukon, and Alaska: Tectonics and metallogeny. *In:* Tectonics, Metallogeny, and Discovery: The North American Cordillera and Similar Accretionary Settings, M. Colpron, T. Bissig, B.G. Rusk and J.F.H. Thompson (eds.), Society of Economic Geologists, https://doi.org/10.5382/SP.17.03.

Norris, D.K., 1985. Eastern Cordilleran foldbelt of Northern Canada: Its structural geometry and hydrocarbon potential. The American Association of Petroleum Geologists Bulletin, vol. 69, no. 5, p. 788–808.

Norris, D.K., 1997. Geological setting. *In:* The Geology, Mineral and Hydrocarbon Potential of Northern Yukon Territory and Northwestern District of Mackenzie, D.K. Norris (ed.), Geological Survey of Canada, Bulletin 422, p. 21–64, https://doi.org/10.4095/208886.

Northwest Territories Geological Survey, 2018. Geological compilation of Canada, NWT portion: Faults. Government of the Northwest Territories, https://ntgs-open-data-ntgs.hub.arcgis.com/datasets/NTGS::nwt-geology-gscmapd1860a/about?layer=0 [accessed 15/05/2025]. .

Pinet, N., 2021. Structural geology of the eastern Richardson Mountains, Yukon and Northwest Territories: Some field observations and a note of caution for palinspastic reconstructions. *In:* Yukon Exploration and Geology 2020, K.E. MacFarlane (ed.), Yukon Geological Survey, p. 1–18.

Poupinet, G., Ellsworth, W.L. and Fréchet, J., 1984. Monitoring velocity variations in the crust using earthquake doublets: An application to the Calaveras fault, California. Journal of Geophysical Research: Solid Earth, vol. 89, no. B7, p. 5719–5731.

Rohr, K.M.M., Lane, L.S. and MacLean, B.C., 2011. Subsurface compressional structures and facies transitions imaged by seismic reflection data, eastern margin of Richardson trough, Peel Plateau, Yukon. Bulletin of Canadian Petroleum Geology, vol. 59, no. 2, p. 131–146.

Rubin, A.M., Gillard, D. and Got, J.-L., 1999. Streaks of microearthquakes along creeping faults. Nature, vol. 400, no. 6745, p. 635–641.

Ruppert, N.A. and West, M.E., 2020. The impact of the USArray on earthquake monitoring in Alaska. Seismological Research Letters, vol. 91, no. 2A, p. 601–610, https://doi.org/10.1785/0220190227.

Scarabello, L., Abdollahzadeh, M., Becker, J. and Pickle, R., 2025. Swiss-seismological-service/scrtdd: v1.8.9. Zenodo, https://doi.org/10.5281/zenodo.16797309.

Schaeffer, A.J., Gosselin, J.M., Audet, P., Cairns, S., Colpron, M. and Elliott, B., 2025. The Western Arctic Regional Network of Seismographs (WARNS): History, challenges, and improvements in continuous broadband seismic data recordings in northwestern Canada. *In:* Yukon Exploration and Geology Technical Papers, 2024, L.H. Weston, A. Stuart, S.K. Schultz, A.D. Brubacher and D.C. Cronmiller (eds.), Yukon Geological Survey, Government of Yukon, p. 51–73.

Schaff, D.P., Bokelmann, G.H., Beroza, G.C., Waldhauser, F. and Ellsworth, W.L., 2002. High-resolution image of Calaveras Fault seismicity. Journal of Geophysical Research, vol. 107, no. B9, 16 p.

Schaff, D.P., Bokelmann, G.H., Ellsworth, W.L., Zanzerkia, E., Waldhauser, F. and Beroza, G.C., 2004. Optimizing correlation techniques for improved earthquake location. Bulletin of the Seismological Society of America, vol. 94, no. 2, p. 705–721.

Shephard, G.E., Müller, R.D. and Seton, M., 2013. The tectonic evolution of the Arctic since Pangea breakup: Integrating constraints from surface geology and geophysics with mantle structure. Earth-Science Reviews, vol. 124, p. 148–183, https://doi.org/10.1016/j.earscirev.2013.05.012.

Stephan, T. and Enkelmann, E., 2025. All aligned on the western front of North America? Analyzing the stress field in the northern Cordillera. Tectonics, vol. 44, no. 9, https://doi.org/10.1029/2025TC009014.

Stephenson, R.A., Dietrich, J.R. and Lane, L.S., 1994. Crustal structure and tectonics of the southeastern Beaufort Sea continental margin. Tectonics, vol. 13, p. 389–400.

Strauss, J.V., Allen, T.J., Malinowski, J., Feng, X., Fraser, T., Melchin, M.J., Taylor, J.F., Day, J., Gill, B.C. and Sperling, E.A., 2020. The Road River Group of northern Yukon, Canada: Early Paleozoic deep-water sedimentation within the Great American Carbonate Bank. Canadian Journal of Earth Sciences, vol. 57, no. 10, p. 1193–1219.

von Gosen, W., Piepjohn, K., McClelland, W.C. and Colpron, M., 2019. Evidence for the sinistral Porcupine shear zone in North Yukon (Canadian Arctic) and geotectonic implications. *In:* Circum-Arctic Structural Events: Tectonic Evolution of the Arctic Margins and Trans-Arctic Links with Adjacent Orogens, K. Piepjohn, J.V. Strauss, L. Reinhardt and W.C. McClelland (eds.), Geological Society of America Special Paper, Geological Society of America, vol. 541, p. 473–491, https://doi.org/10.1130/2019.2541(21).

Waldhauser, F., 2001. HypoDD: A computer program to compute double-difference earthquake locations. Open-File Report 01-113. US Geological Survey, https://doi.org/10.3133/ofr01113.

Waldhauser, F. and Ellsworth, W.L., 2000. A double-difference earthquake location algorithm: Method and application to the northern Hayward fault, California. Bulletin of the Seismological Society of America, vol. 90, no. 6, p. 1353–1368, https://doi.org/10.1785/0120000006.

Waldhauser, F. and Schaff, D.P., 2008. Large-scale relocation of two decades of northern California seismicity using cross-correlation and double-difference methods. Journal of Geophysical Research, vol. 113, no. B8, https://doi.org/10.1029/2007JB005479.

Wolfe, C.J., 2002. On the mathematics of using difference operators to relocate earthquakes. Bulletin of the Seismological Society of America, vol. 92, no. 8, p. 2879–2892.

Yukon Geological Survey, 2016. A Geological Compilation Map of the Yukon Territory Intended for Use by the Exploration Community, Prospectors and Geologists: Faults. GeoYukon, Government of Yukon, https://yukon.maps.arcgis.com/home/item.html?id=2695ad28cb2c421a95112313397b844d [accessed 15/05/2025].